Oxygen Reduction Reaction and Hydrogen Evolution Reaction Catalyzed by PdRu Nanoparticles Encapsulated in Porous Carbon Nanosheets

Juntai Tian,[a,#] Wen Wu,[a,#] Zhenghua Tang,[,a,b] Yuan Wu,[c] Robert Burns,[d] Brandon Tichnell,[d] Zhen Liu,[d] and Shaowei Chen[a,e]*

[a] *Guangzhou Key Laboratory for Surface Chemistry of Energy Materials, New Energy Research Institute, School of Environment and Energy, South China University of Technology, Guangzhou Higher Education Mega Centre, Guangzhou, 510006, China.*

E-mail: zhht@scut.edu.cn

[b] *Guangdong Provincial Key Laboratory of Atmospheric Environment and Pollution Control, Guangdong Provincial Engineering and Technology Research Center for Environmental Risk Prevention and Emergency Disposal, South China University of Technology, Guangzhou Higher Education Mega Centre, Guangzhou, 510006, China*

[c] *Department of Clinical Medicine, Fuzhou Medical College of Nanchang University, Fuzhou, Jiangxi 344000, China*

[d] *Department of Physics & Engineering, Frostburg State University, Frostburg, MD 21532-2303, United States.*

[e] *Department of Chemistry and Biochemistry, University of California, 1156 High Street, Santa Cruz, California 95064, United States.*

#: These authors contributed equally.

Table S1. The summary of the ORR performance and size of the samples with different Pd-to-Ru ratios (The total metal mass loading was set as 10%).

Sample	Molar ratio of Pd: Ru	Size (nm)	E_{onset} (V vs. RHE)	$E_{1/2}$ (V vs. RHE)	Diffusion-limited current density @ +0.3 V (mA cm^{-2})
Ru_{100}/CNs	1: 0	1.55 ± 0.57	0.841	0.764	-3.27
$Pd_{33}Ru_{67}$/CNs	1: 2	1.94 ± 0.40	0.877	0.791	-4.26
$Pd_{50}Ru_{50}$/CNs	1: 1	3.67 ± 0.96	0.903	0.799	-5.14
$Pd_{67}Ru_{33}$/CNs	2: 1	5.90 ± 1.02	0.895	0.804	-3.99
Pd_{100}/CNs	0: 1	3.76 ± 0.99	0.877	0.813	-3.43
Pd/C	/	/	0.915	0.816	-3.67

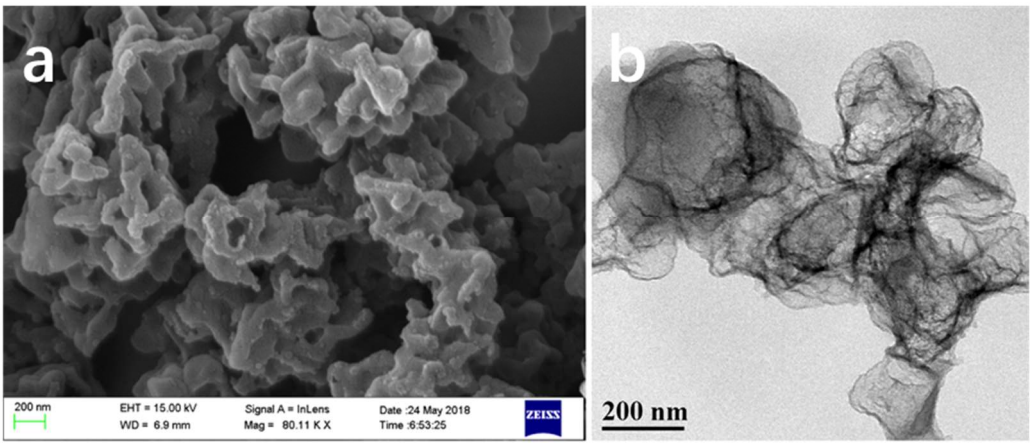

Figure S1. (a) The typical SEM and (b) TEM images of porous carbon nanosheets.

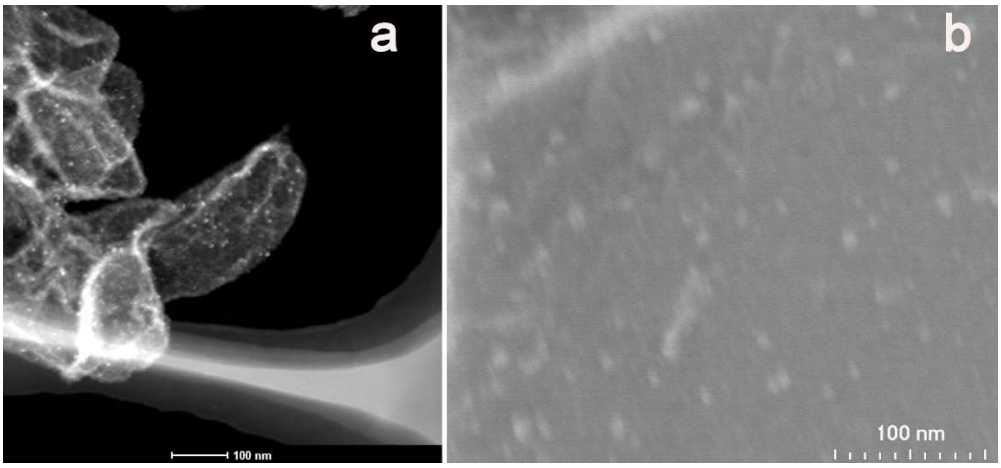

Figure S2. (a) The typical high-angle annular dark field-scanning tunneling electron microscopy (HAADF-STEM) and (b) Scanning electron microscopy (SEM) images of $Pd_{50}Ru_{50}$/CNs.

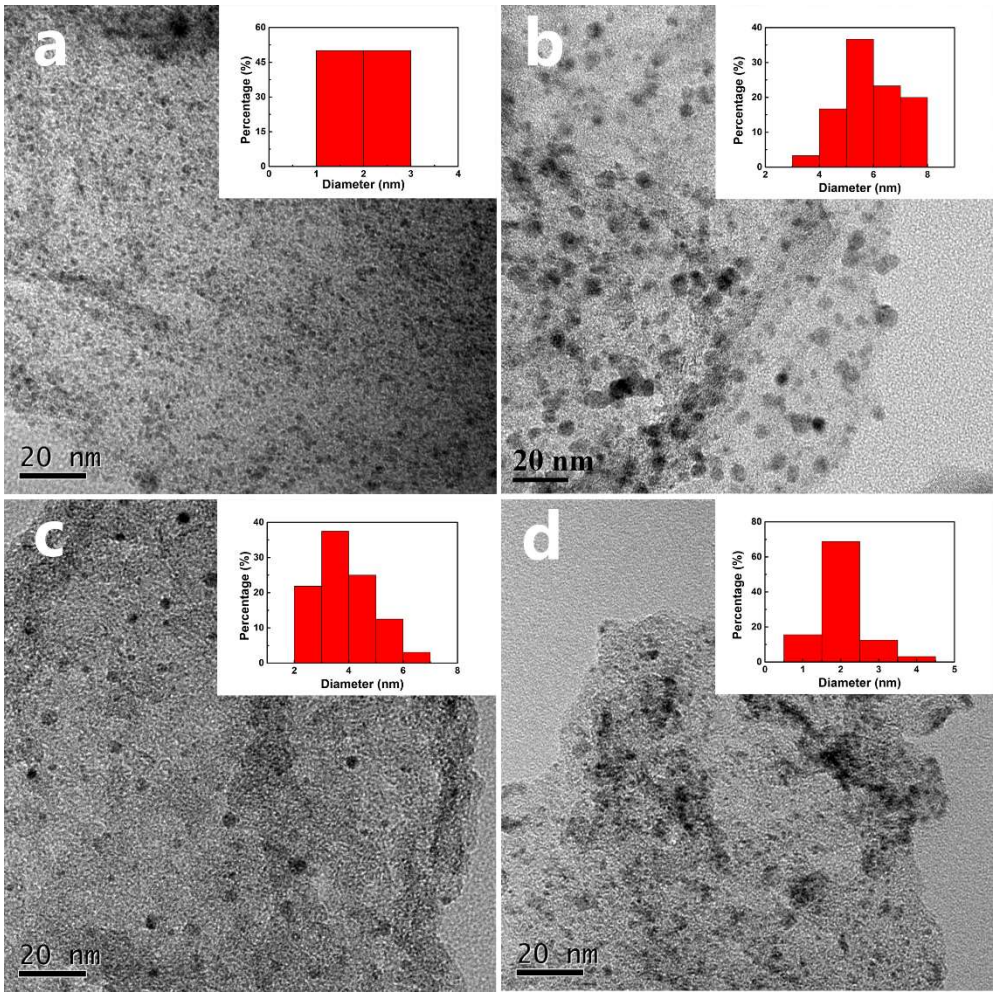

Figure S3. The representative TEM images of (a) $Pd_{33}Ru_{67}$/CNs (1.94 ± 0.40 nm), (b) $Pd_{67}Ru_{33}$/CNs (5.90 ± 1.02 nm), (c) Pd_{100}/CNs (3.76 ± 0.99 nm) and (d) Ru_{100}/CNs (1.55 ± 0.57 nm). (Inset is the corresponding size distribution histogram).

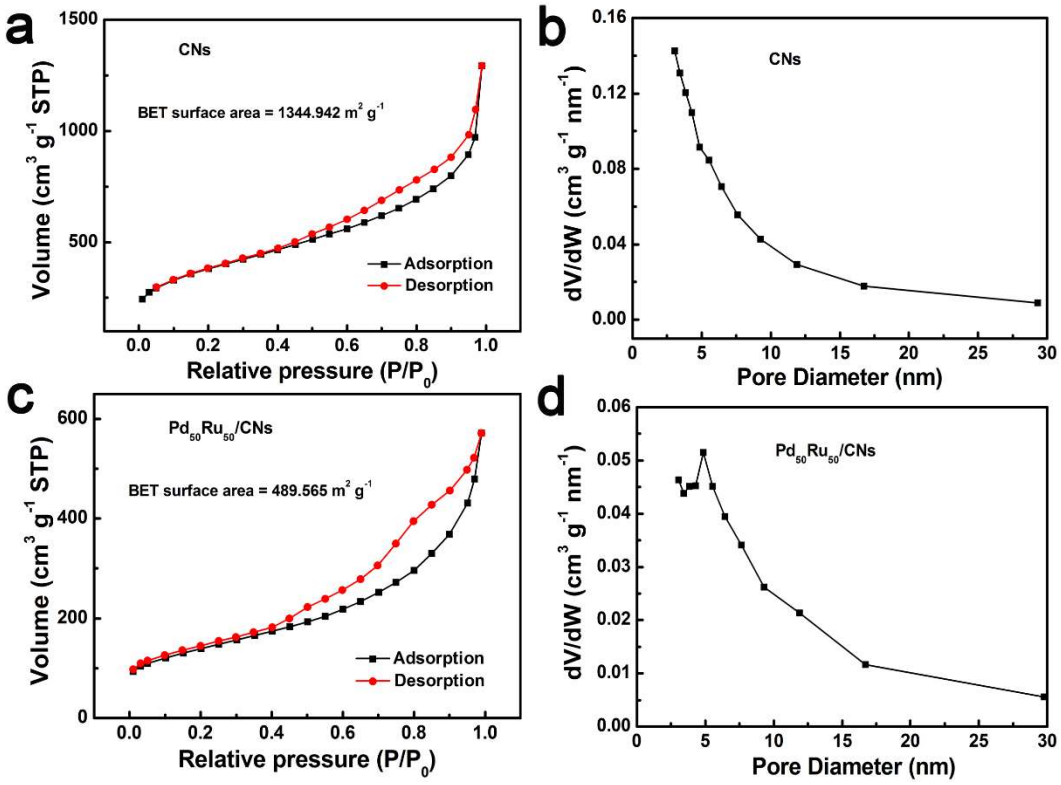

Figure S4 (a, c) Nitrogen adsorption/desorption isotherms at 77 K and (b, d) the corresponding pore-size distribution of CNs and $Pd_{50}Ru_{50}$/CNs.

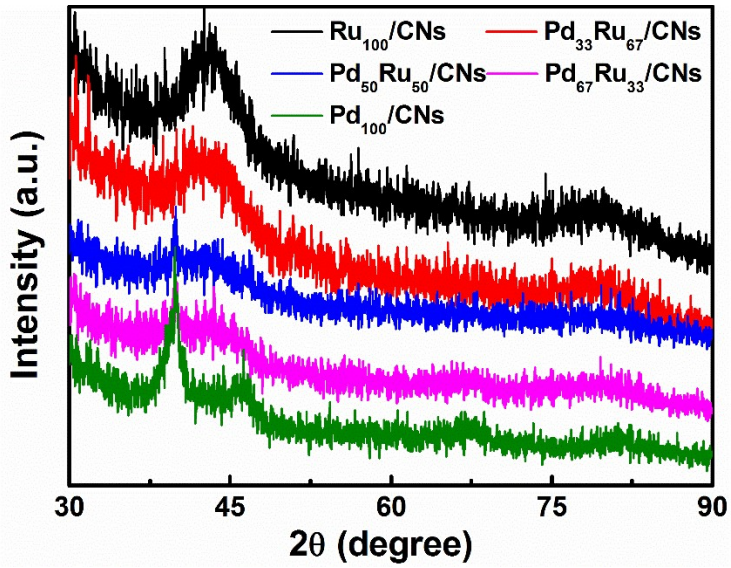

Figure S5. The XRD patterns of all the samples.

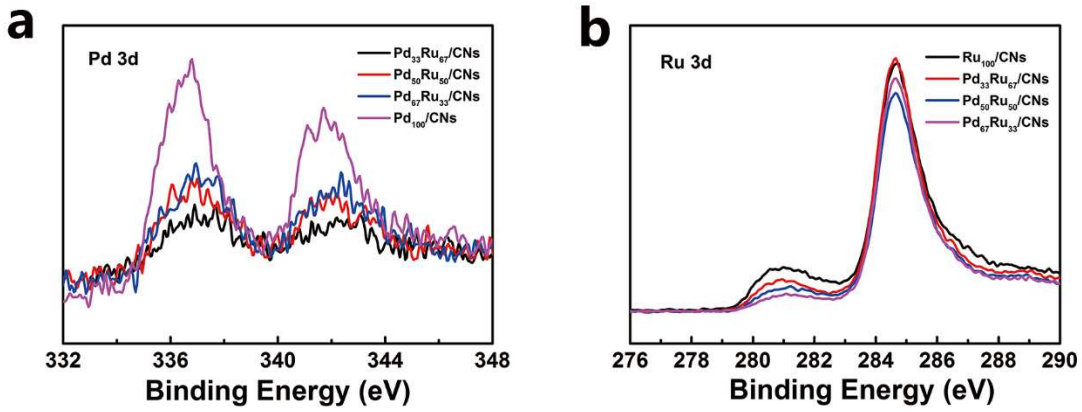

Figure S6. The high-resolution XPS spectra of the (a) Pd3d and (b) Ru3d electrons in the series of samples.

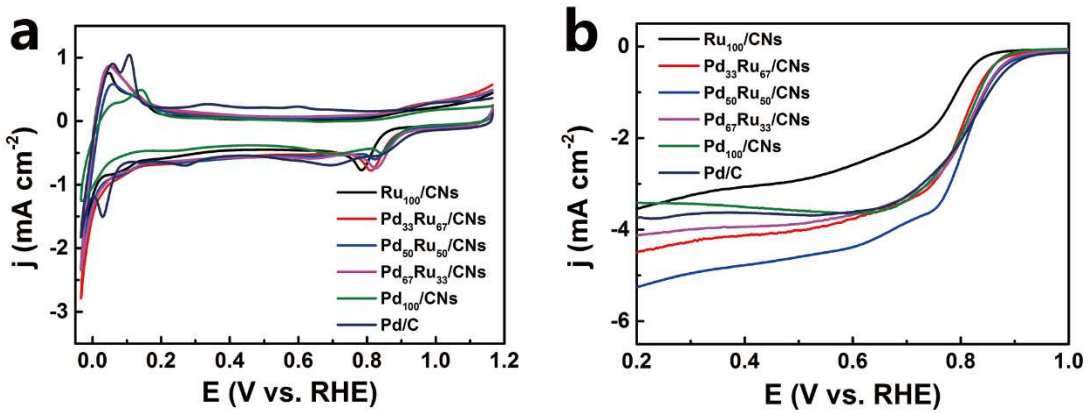

Figure S7. (a) The CV curves and (b) RRDE voltammograms of all the Pd_xRu_{100-x}/CNs alloyed samples and Pd/C in O_2-saturated 0.1 M KOH solution.

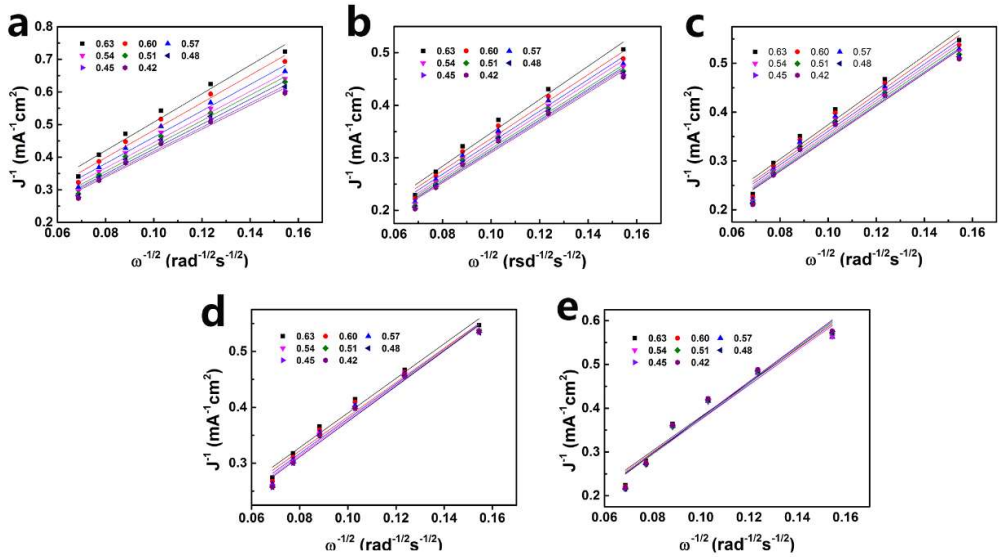

Figure S8. The Koutecky-Levich (K-L) plots of (a) Ru_{100}/CNs, (b) $Pd_{33}Ru_{67}$/CNs, (c) $Pd_{67}Ru_{33}$/CNs, (d) Pd_{100}/CNs and (e) Pd/C.

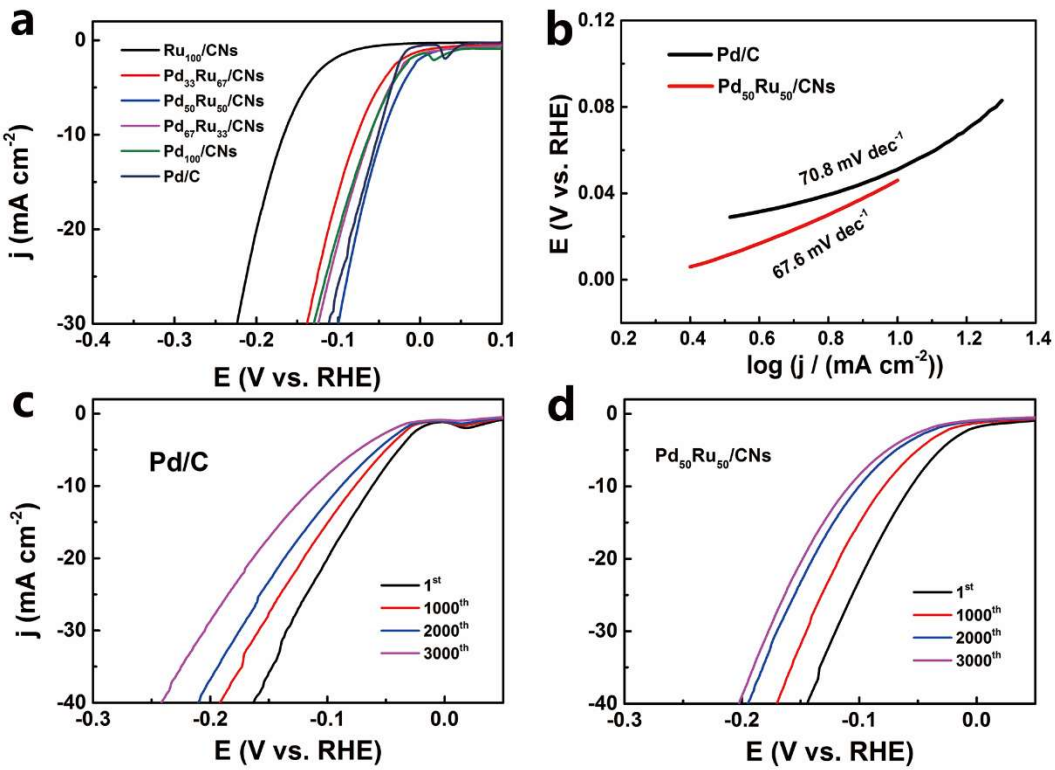

Figure S9. HER activity curves (a) of PdRu alloy CNs and Pd/C in 0.5 M H_2SO_4 with scan rate of 10 mV s^{-1}. The corresponding Tafel plots (b) of the $Pd_{50}Ru_{50}$/CNs and Pd/C catalyst. Polarization curves after continuous potential sweeps of Pd/C (c) and $Pd_{50}Ru_{50}$/CNs (d) at 100 mV s^{-1} in 0.5 M H_2SO_4.